

Multiparticle Beam Dynamics Simulations for ASTA using PARMELA Code*

Yuan Hui Wu

Department of Physics, University of Massachusetts Amherst , Amherst , Massachusetts, 01003, USA

Tanaji Sen

Accelerator Physics Center, Fermi National Accelerator Laboratory, Batavia, 60510, USA

Philippe Piot

Fermi National Accelerator Laboratory and Northern Illinois University, Batavia, 60510, USA

(Dated: August 24, 2012)

The Advanced Superconducting Test Accelerator (ASTA) under construction at Fermilab will generate up to $2E10$ electrons per bunch. The collective effects and space charge effects created by low energy electrons have a large impact on beam emittance and size. In this research project, we used a simulation code Phase and Radial Motion in Electron Linear Accelerators (PARMELA) developed in Los Alamos National Laboratory for beam dynamic simulation. We optimize the parameters of the solenoidal field on the photocathode, the rf gun field, the fields and phases of the two accelerating cavities and the third harmonic cavity with and without space charge effects. Bunch compression after the first bunch compressor is also optimized with and without space charge.

I. INTRODUCTION

Over the last decade, Fermilab has played an important role in photoinjector R&D and application to advanced accelerator R&D. The Advanced Superconducting Test Accelerator (ASTA) facility at Fermilab is under development at the New Muon Lab (NML) at Fermilab. The potential use of ASTA will aim to support both Project X, International Linear Collider (ILC) and other advanced acceleration R&D experiments[1].

FIG.1 shows a schematic of the ASTA beamline which consists of a photocathode located before the RF gun. The Photocathode is illuminated with a laser pulse, emitting low transverse emittance electron beam. The RF gun

is surrounded by two solenoid magnets. The magnetic field created by two solenoid will be used to reduce the transverse beam size of electrons. The beam from a photo-emission electron source will be accelerated by a RF gun cavity and two superconducting cavities (CAV1 and CAV2) [2]. A third harmonic superconducting cavity (CAV39) is designed to linearize the longitudinal phase space and as a consequence decelerates the electrons by a few MeV. The green rectangles along the transportation line represent the quadrupole channel used to focus and stabilize the beam. A magnetic bunch compressor (BC1), which is made up of four dipole magnets, is used to compress the bunch longitudinally. After BC1 the beam can be directed either through a dogleg to experimental area or injected into the next accelerating module.

The designed frequency of ASTA photoinjector gun is 1.3 GHz, the accelerating length of the gun is 0.265m and the average accelerating field is 23.67 MV/m. It is capable of accelerating the beam to ~ 4.6 MeV. Two solenoid magnets surround the RF gun and are powered to have zero magnetic field at the photocathode and also to reduce the transverse emittance growth due to the Rf gun and space charge. Superconducting cavities CAV1 and CAV2 are 9-cell 1.3 GHz superconducting RF cavities that can accelerate electron to ~ 45 MeV downstream. CAV2 also introduces a properly correlated energy spread (i.e. a chirp) so that the bunch can be compressed in BC1. The third harmonic 3.9 GHz superconducting cavity CAV39 was proposed by DESY for a new generation of high brightness photoinjector. It is used to linearize the longitudinal phase space following the curvature induced by the upstream cavities.

A beam dynamics model of the ASTA photoinjector was implemented by ASTRA code previously [2]. The beam dynamics simulations from PARMELA is used to compare with ASTRA. In this project, we simulated ASTA beamline from the photocathode to BC1. We find the parameters (phase of CAV2, voltage and phase of

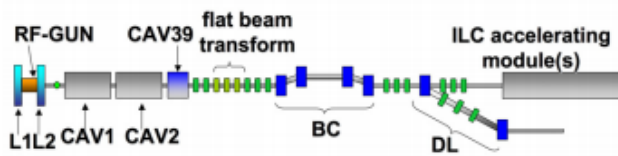


FIG. 1: Schematic of ASTA photoinjector, L1 and L2 are two solenoid magnets surrounding a 1.5 cell rf gun. Electrons were excited by a laser beam hit on the photocathode, the generated electrons travel along the magnetic field of the solenoid as it undergoes acceleration within the RF gun. CAV1, CAV2 and CAV39 are 9 cells superconducting cavity which operating at 1.3GHz and 3.9GHz. The green rectangles is the quadrupole channel which consists of 8 quadrupoles. BC1 is the first bunch compressor chicane and the downstream accelerating cryomodules consist of eight 9 cells superconducting cavities.

*This work was supported by the Fermi Research Alliance and Lee Teng summer intern program. email: yuanhuiw@yaho.com

TABLE I: Initial electron bunch generation conditions.

Value	Unit	Description
3.2	nano-Coulomb	Bunch charge
3	ps	Bunch length
0	keV	Energy spread

TABLE II: ASTA beamline elements position (from cathode) and parameters

Position	length	Description
0m	0.265m	RF gun cavity
1.7672m	1.3492m	CAV1
4.6540m	1.3492m	CAV2
7.1701m	0.5059m	CAV3.9
8.0162	0.167m	QUAD 1
8.2190m	0.167m	QUAD 2
8.8285m	0.167m	QUAD 3
9.2106m	0.167m	QUAD 4
9.5927m	0.167m	QUAD 5
10.1396m	0.167m	QUAD 6
10.3404m	0.167m	QUAD 7
10.5412m	0.167m	QUAD 8
11.1960m	0.2m	Dipole 1
11.7409m	0.128m	Small QUAD 1
12.1634m	0.2m	Dipole 2
12.8072m	0.128m	Small QUAD 2
13.1814m	0.2m	Dipole 3
13.6759m	0.128m	Small QUAD 3
14.1488m	0.2m	Dipole 4

CAV39) that minimize the linearize longitudinal phase space and minimize the bunch length, and optimize the solenoidal field that minimize the space charge related emittance growth after BC1.

II. RF CAVITY ACCELERATION

The beam energy after a rf cavity with peak voltage V and phase ϕ is calculated using

$$E(z) = eV \cos(\phi + kz) \quad (1)$$

where z is the longitudinal position of a particle with respect to the reference particle and k is wave number ($k = \frac{2\pi}{\lambda}$). Since cosine function is maximum when $\phi=0$, when $z=0$, the rf phase equal to 0 for the maximum en-

ergy gain (on crest). Expanding equation (1) we find

$$E(z) = eV \cos(\phi) - eV k \sin(\phi) z - \frac{1}{2} eV k^2 \cos(\phi) z^2 + \mathcal{O}(z^3) \quad (2)$$

The ASTA beamline consists of 4 cavities, namely the rf gun cavity, CAV1, CAV2 and CAV39. The beam is on-crest in the rf gun and CAV1 for maximum energy gain. The rf phase for CAV2 is off crest, rf phase and peak voltage for CAV39 are calculated to linearize the longitudinal phase space

III. SPACE CHARGE EFFECT

Space charge effects are one of the main topics studied in this project. After electrons generated from the photocathode, the low energy electrons in the photoinjector have high space charge forces. ASTRA and PARMELA are two beam dynamics simulation codes which broadly used for electron accelerators. The PARMELA simulation code includes space charge and image space charge calculating routines, It is capable of calculating 2D and 3D space charge effects.

IV. OPTIMIZATION PROCEDURES

To optimize the parameters for ASTA, we divided the optimization procedures into steps. Parameters for elements along the beam line need to be optimized for maximum performance. Because space charge involves complicate phenomena and results are difficult to predict, to test our code is working properly, we started our simulation first without space charge and studied the case with space charge.

A. Solenoid Magnetic field

To minimize the transverse emittance of electron beam after it is generated from the photocathode, the magnetic field of the solenoid needs to be optimized for both with and without space charge. In our system, two solenoid magnets surround the RF gun cavity, the magnetic field of the solenoid magnets have different fields and are opposite to each other so that the combined magnetic field strength is zero at the photocathode surface and non-zero after the photocathode. We scan a range of magnetic fields in the middle of rf gun cavity and plot the beam transverse emittance at the entrance of first quadrupole. We concluded that the magnetic field $B \sim 1668.723$ gauss without space charge and ~ 1776.094 gauss with space charge will result in the lowest transverse emittance.



FIG. 2: Superconducting 1.3 GHz and 3.9GHz 9-cell cavity for the ASTA [8]

B. On Crest for RF Gun Cavity and CAV1

In our definition, particles are on-crest in the rf wave when the phase $\phi = 0$. Because each cavity is located at different longitudinal positions, we need to optimize the RF phase for each RF cavity for maximum energy. Since the code PARMELA does not automatically determine the on-crest phase, we search for a phase which results in the highest energy. We assume the on crest phases are the same both with and without space charge. The on crest phases for CAV1 and CAV2 in PARMELA are 141 and 153 degrees respectively.

The peak gradient for CAV1 and CAV2 is 35 MV/m, and total length is 134.92 cm. Because the effective length in which particles are accelerated is 100cm and the average voltage is 22MeV/m, the peak energy gain in CAV1 and CAV2 is ~ 22 MeV.

C. Off Crest for CAV2

The bunch needs to be off-crest in CAV2 so that particle in the tail have a higher energy than particles at the head. This allows the tail particle to travel a shorter path in the bunch compressor and catch up with the head. The off-crest phase in CAV2 is determined by the requirement of maximum bunch compression and is approximated by

$$\phi_3 = \phi_{3,0} + \Delta\phi_3 \quad (3)$$

where,

$$\phi_{3,0} = \sin^{-1}\left(\frac{E_0}{eV_3 k |R_{56}|}\right) \quad (4)$$

$$\Delta\phi_3 = -\frac{k}{k_4} \frac{V_1 + V_2 + V_3}{V_3 \cos(\phi_{3,0})} \left[1 - \left(\frac{V_1 + V_2 + V_3 \cos(\phi_{3,0})}{V_1 + V_2 + V_3}\right)^2\right]^{1/2} \quad (5)$$

E_0 is the particle energy exiting from CAV2. V_1 , V_2 and V_3 are the peak accelerating voltage in the rf gun, CAV1 and CAV2 respectively. R_{56} is the longitudinal dispersion in BC1 which for ASTA has been set to -0.19m. The

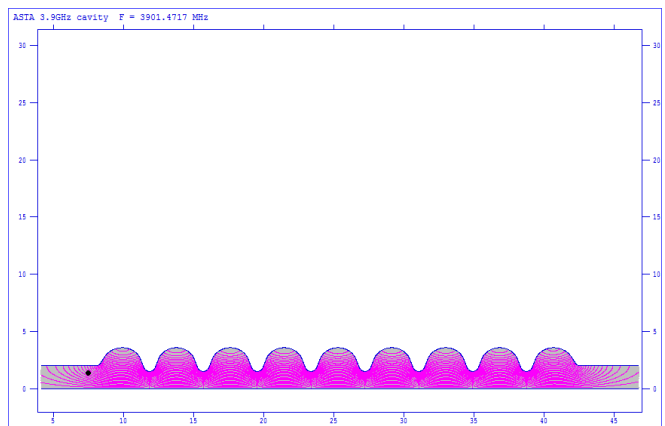


FIG. 3: Superfish model for 3.9GHz superconducting cavity

symbol k is the wave number of 1.3GHz cavity and k_4 is the wave number of 3.9GHz cavity.

D. CAV39

CAV39 is a 3.9 GHz cavity used to linearize the longitudinal phase space. CAV39 has a length of 0.5 meter and has a peak gradient 14 MV/m [9]. A model of CAV39 needed to be developed for input into PARMELA. FIG. 3 shows the schematic cross-section of the cavity cells generated using the Superfish program from the dimensions provided by T. Khabibouline (FNAL). In order to linearize the phase space, the quadratic correlation is removed. The voltage V_4 and phase ϕ_4 of CAV39 can be calculated by

$$V_4 = \frac{k^2}{(k_4)^2} (V_1 + V_2 + V_3) \quad (6)$$

$$\phi_4 = \pi + \cos^{-1}\left[\frac{V_1 + V_2 + V_3 \cos(\phi_{3,0})}{V_1 + V_2 + V_3}\right] \quad (7)$$

E. Quadrupole Channel

In between CAV39 and the first bunch compressor BC1, there are 8 quadrupoles, each quadrupole with a length of 0.16 m. The individual quadrupoles have different strengths and was optimized by another simulation code (Elegant) by Chris Prokop from Northern Illinois University (NIU). The initial values of the Twiss functions at the entrance of the first quadrupole as determined by PARMELA were given as input to Elegant and used to match to the desired Twiss functions in BC1. This was done both with and without space charge. Table III and table IV show the values of the quadrupole strengths found for these two cases.

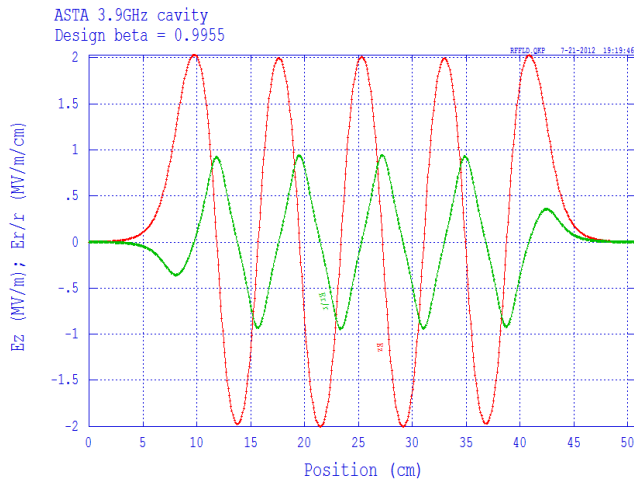


FIG. 4: Accelerating gradient for 3.9GHz superconducting cavity. The red curve is the longitudinal electric field along the cavity, and the green curve is the transverse electric field along the cavity.

TABLE III: Quadrupole strengths use in each quadrupoles without space charge. Quads 3, 4, and 5 are skew quads and are turned off.

Value	Unit	Description
42.58	Gauss/cm	QUAD 1
38.45	Gauss/cm	QUAD 2
0	Gauss/cm	QUAD 3
0	Gauss/cm	QUAD 4
0	Gauss/cm	QUAD 5
10.078	Gauss/cm	QUAD 6
-98.00	Gauss/cm	QUAD 7
50.70	Gauss/cm	QUAD 8

F. Bunch Compressor and Coherent Synchrotron Radiation

In order to produce high brightness electron beams with high peak current, the generated bunch will be accelerated to energies where the space charge forces are sufficiently low. To compress the bunch longitudinally, the bunch is properly chirped in CAV2. Compression can be achieved in the bunch compressor when the head and tail of the bunch encounter different phases and the head has lower energy than the bunch tail.

FIG 5 shows a schematic of the bunch compressor which is composed of 4 dipoles and the parameters for them are listed on table VII. As electrons pass through the four 20cm long dipoles with bending angles -18, +18, +18 and -18 respectively, the bending trajectory created by dipoles can cause electron bunches to emit coherent synchrotron radiation (CSR). The energy radiated can disturb the electron bunches and increase the en-

TABLE IV: Quadrupole strengths with space charge. The strengths are stronger than in the case with no space charge.

Value	Unit	Description
-94.50	Gauss/cm	QUAD 1
98.19	Gauss/cm	QUAD 2
0	Gauss/cm	QUAD 3
0	Gauss/cm	QUAD 4
0	Gauss/cm	QUAD 5
105.80	Gauss/cm	QUAD 6
-155.4	Gauss/cm	QUAD 7
48.31	Gauss/cm	QUAD 8

TABLE V: No space charge: optimization parameters in PARMELA for ASTA from the RF gun cavity to bunch compressor BC1.

Value	Unit	Description
1660	gauss	Magnetic field of solenoid magnet
355.2	degree	On crest phase RF gun
332	degree	On crest phase CAV1
26.254	MeV	Energy after CAV1
127	degree	off crest phase CAV2
4	degree	Off crest phase CAV39
47.528	MeV	Energy after CAV2
43.043	MeV	Energy after CAV39

ergy spread and transverse emittance. Since the current version of PARMELA is not capable of calculating CSR effects, our simulations result do not include CSR effects.

TABLE VI: With space charge: optimization parameters for ASTA in PARMELA from the RF gun cavity to bunch compressor BC1.

Value	Unit	Description
1776.094	gauss	Magnetic field of solenoid magnet
355.2	degree	On crest phase RF gun
332	degree	On crest phase CAV1
26.254	MeV	Energy after CAV1
127	degree	on crest phase CAV2
16	degree	Off crest phase CAV39
47.447	MeV	Energy after CAV2
43.498	MeV	Energy after CAV39

TABLE VII: Parameter for 4 dipoles bunch compressor

Value	Unit	Description
0.30124	meter	Bending dipole length (L_{dip})
0.68	meter	Drift between 1st and 2nd dipole (L_{12})
1.1125	meter	Drift between 2nd and 3rd dipole (L_{23})
0.68	meter	Drift between 3rd and 4th dipole (L_{34})
18	degree	Bending angle (θ)
0.19	meter	Momentum compaction (R_{56})
3.38111	meter	projected length of chicane(L)

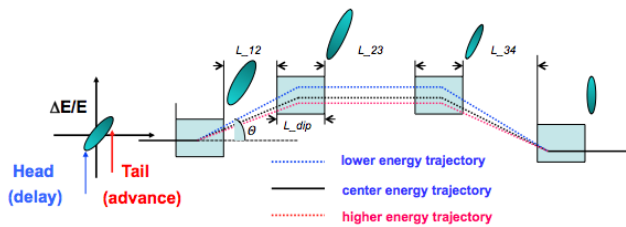


FIG. 5: 4-bending magnet chicane. The electron beam passes through a region where the path length is energy dependent. The different path lengths through a dispersive section can compress the bunch length.

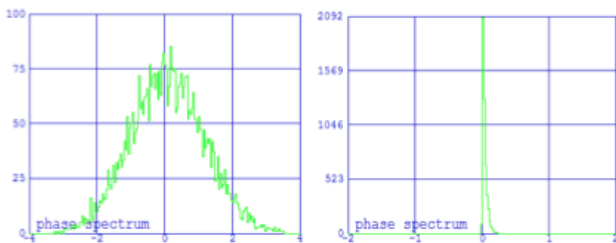


FIG. 6: Simulation result with PARMELA without space charge: the longitudinal current profile before and after the bunch compressor. the electron bunch length is compressed from 3ps to 0.07ps.

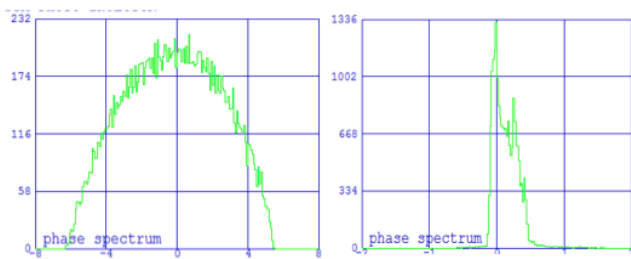


FIG. 7: Simulation result with PARMELA with space charge: the longitudinal current profile before and after the bunch compressor. the electron bunch length is compressed from 3ps to 0.39ps.

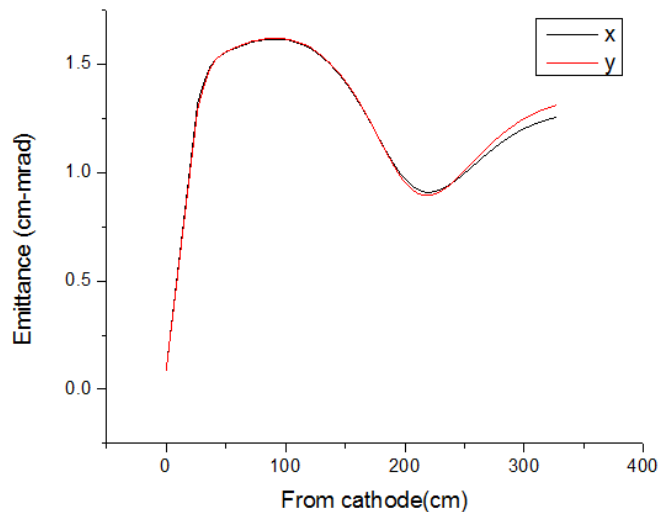


FIG. 8: Normalized rms transverse emittance oscillations in the drift space after rf gun cavity.

V. EMITTANCE OSCILLATION SIMULATION AT DRIFT SPACE

In the region after the RF gun cavity, the generated electrons have low energy and experience high space charge forces. Some theories and experimental results have shown that the emittance is oscillating throughout the drift space in the space charge dominated regime [10]. Using PARMELA, we using the same setup to simulate the transverse emittance of 3.2 nano-Coulomb electron bunches in a drift space with a length of 3 meters, see FIG.8. The lowest transverse emittance can be attained at $\sim 2m$ from the cathode with transverse emittance ~ 0.8 mm-mrad. The simulation provides some information on where CAV1 should be located for the lowest emittance.

VI. RESULTS

We perform the optimization without space charge, and then with space charge. The idea behind this is we first want to check that the PARMELA simulation has similar results (such as Courant-Snyder Twiss functions, on crest phase and off crest phase etc) as other simulation codes without space charge, and then we consider optimizing the parameters with space charge.

The average voltage gradient and phase are optimized for each elements. For the case without space charge see table V. For the case with space charge see table VI. Using these settings, the program generated the longitudinal phase space in each elements, see FIG 9 and FIG 10. FIG 11 and 12 are plots of the beta functions and FIG 13 and 14 show the rms beam size evolution along the beamline.

Initially electrons were generated from the photocath-

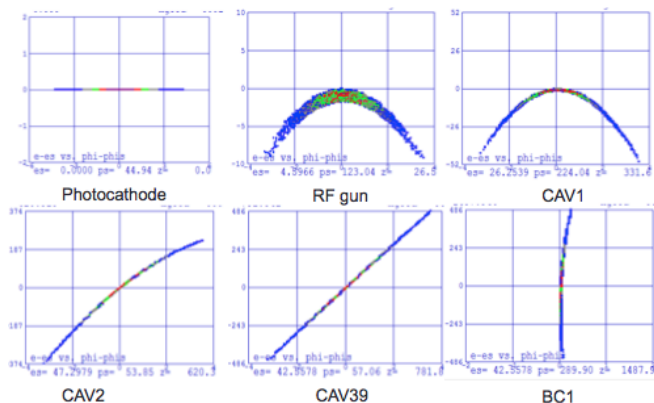


FIG. 9: Longitudinal phase space in different elements without space charge. Top row shows the longitudinal phase space at the positions of the photocathode, after the rf gun and CAV1. The bottom row shows the longitudinal phase space after CAV2, CAV39 and BC1. For the RF gun cavity and CAV1, the phases are on crest. In the absence of space charge, the the head and tail of the electron bunch gain less energy than the center of the bunch. For CAV2, the phase is off crest and longitudinal phase space is rotated because the tail gains more energy than the head of the electron bunch in the RF accelerating field. After BC1, the electron bunch is compressed from 3ps to 0.07ps, with a compression factor of 42.1.

ode with bunch length of 3ps and no energy spread. The longitudinal phase is distributed along the horizontal axis. The longitudinal phase space without space charge after the RF gun and CAV1 has a parabolic shape and this is because we set the phases of rf gun and CAV1 to be on crest, the tail and head of the electron bunch are off crest and gain less energy compared with the electrons in the center of the bunch. For the case with space charge, the longitudinal phase space is complicated by the space charge forces, the repulsive electric force changes the electrons trajectory and lengthens the electron bunch. In the longitudinal phase space after RF gun and CAV1, we saw that the head of the bunch gains energy while the tail of the bunch loses energy with the mean energy staying he same.

After BC1, the bunch length is compressed from 3ps to 0.07ps without space charge, and compressed from 3ps to 0.39ps with space charge. The longitudinal phase space with space charge after BC1 demonstrates an irregular shape at the head and the tail of the bunch. The distortion can be caused by space charge induced nonlinear beam dynamics.

The optimized parameters for solenoid current, phase of CAV2, phase and voltage of CAV39 and the quadrupole strength are different without space charge and with space charge. Before the electron bunch enters the quadrupole channel, the alpha and beta functions are different with space charge. Because we use the initial alpha and beta functions to determine strength of individual quadrupoles, this leads to differences in the Twiss functions and rms beam size for the two cases.

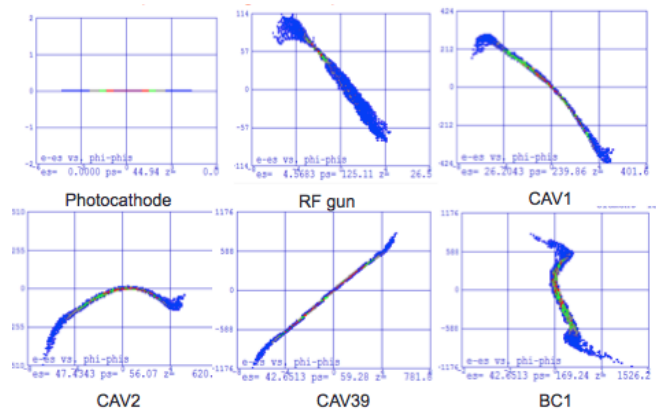


FIG. 10: Longitudinal phase space in different elements with space charge. Top row: longitudinal phase space at the positions of the photocathode, after the rf gun and CAV1. Bottom row: longitudinal phase space after CAV2, CAV39 and BC1. The parameters for each element are optimized and the electron bunch is compressed from 3ps to 0.39 ps, with a compression factor of 7.77.

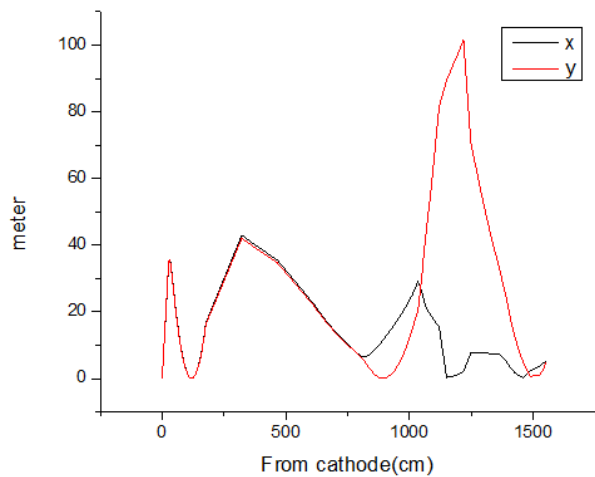


FIG. 11: No space charge: Courant-Snyder β functions in the x and y directions.

VII. CONCLUSION

In this project, we have optimized parameters for the gun cavity, CAV1, CAV2, CAV39 and the bunch compressor to minimize space charge related emittance growth and maximize bunch compression. Without space charge, the chicane can compress the electron bunch from initial length of 3ps to 0.07ps with a compression factor of 42.09. With space charge, the bunch length can be compressed from 3ps to 0.39 ps with compression factor of 7.77. The normalized emittance after BC1 is ~ 7.8 mm with space charge, and is ~ 1.3 mm without space charge.

We have observed differences in longitudinal phase space with and without space charge. Space charge ef-

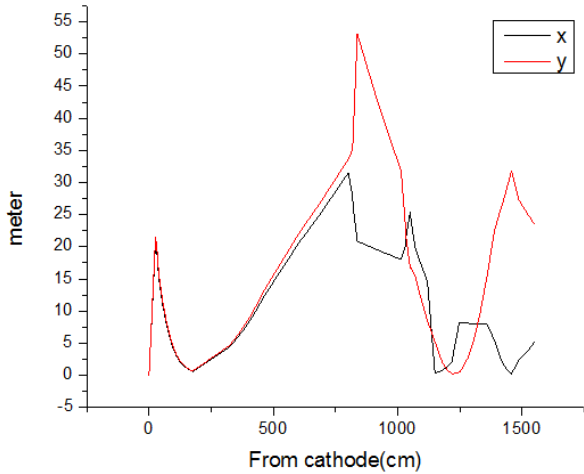


FIG. 12: With space charge: Courant-Snyder β functions in the x and y directions.

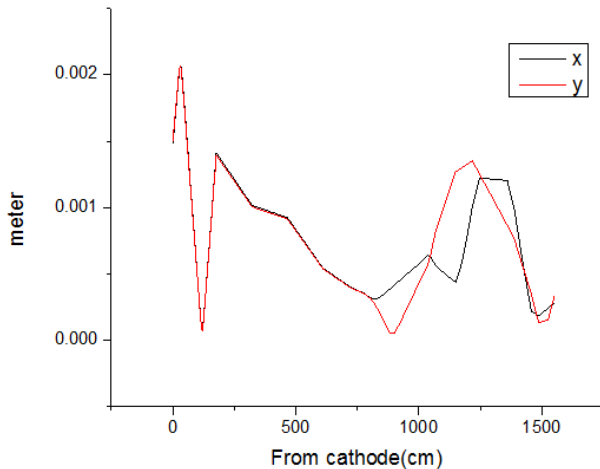


FIG. 13: No space charge: beam size in the x and y directions from photocathode to the bunch compressor BC1.

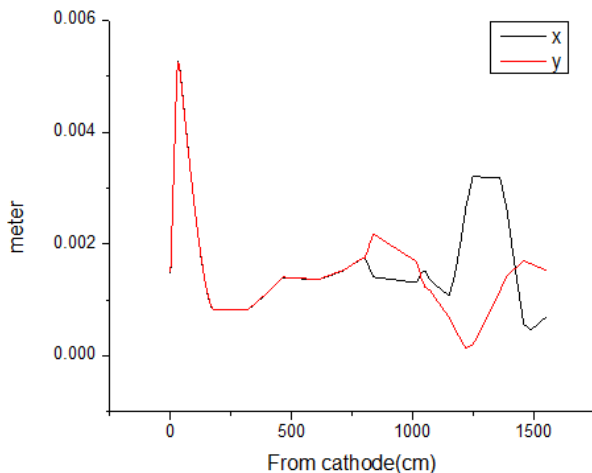


FIG. 14: With space charge: beam size in the x and y directions from the photocathode to the bunch compressor BC1.

fects limited the performance of the bunch compressor, introduced the irregularity of longitudinal phase space along the ASTA beamline and increased the transverse emittance.

VIII. FUTURE WORK

Further study requires implementing the CSR effect in BC1 using PARMELA, and adding the remaining ASTA beamline elements including the 2nd bunch compressor. It would be useful to compare our simulations with other beam dynamics codes such as TRACK and IMPACT. These simulations can then be bench-marked against each other and against measurements which could also add more confidence in the predictive power of the simulations. Since different beam dynamics codes employ different algorithms and methods, this usually leads to some codes with better predictive power than others. Furthermore, not all codes model all of the important effects so it is necessary to combine different codes, e.g. PARMELA can model the low energy space charge and rf effects starting from the photocathode and the output particle distribution at the entrance to the first bunch compressor could be used as input into Elegant to study CSR effects.

IX. ACKNOWLEDGMENTS

The first author would like to express his sincere appreciation to his advisors, Tanaji Sen and Philip Piot whose advice, support and direction made this project possible, and to Daniel Mihalcea and Chris Prokop from NIU who taught him how to use PARMELA and provided him with research resources. Also, he would like to thank Eric Prebys for organizing this program and making this internship very memorable.

-
- [1] "Report on Workshop on Future Directions for Accelerator R&D at Fermilab" May 11-13, 2009 Lake Geneva, WI.
- [2] P. Piot, Y-E Sun and M. Church "Beam Dynamics Simulations of the NML Photoinjector at Fermilab" THPD020, Proceedings of IPAC10, Kyoto, Japan.
- [3] I. S. Ko, W.Chou "Beam Dynamics Newsletter " International Committee for Future Accelerators , December 2005.
- [4] L. M. Young "PARMELA" Los Alamos National Laboratory report LA-UR-96-1835 (Revised April 22, 2003).
- [5] J. H. Billen and L. M. Young "Poisson Superfish" Los Alamos National Laboratory report LA-UR-96- 1834 (Revised February 6, 2003).
- [6] C.M. Ginsburg , T. Arkan, S. Barbanotti, H. Carter, M. Champion, L. Cooley, C. Cooper, M. Foley, M. Ge, C. Grimm, E. Harms, A. Hocker, R. Kephart, T. Khabiboulline, J. Leibfritz, A. Lunin, J. Ozelis, Y. Pischalnikov, A. Rowe, W. Schappert, D. Sergatskov, A. Sukhanov, G. Wu "1.3 GHz Superconducting rf Cavity Program at Fermilab" Fermilab-conf-11-132-td.
- [7] Aune, B., R. Bandelmann, D. Bloess, B. Bonin, A. Bosotti, M. Champion, C. Crawford, G. Deppe, B. Dwersteg, D. A. Edwards, H. T. Edwards, M. Ferrario, M. Fouaidy, P.-D. Gall, A. Gamp, A. Gssel, J. Graber, D. Hubert, M. Hning, M. Juillard, T. Junquera, H. Kaiser, G. Kreps, M. Kuchnir, R. Lange, M. Leenen, M. Liepe, L. Lilje, A. Matheisen, W.-D. Mller, A. Mosnier, H. Padamsee, C. Pagani, M. Pekeler, H.-B. Peters, O. Peters, D. Proch, K. Rehlich, D. Reschke, H. Safa, T. Schilcher, P. Schmsers, J. Sekutowicz, S. Simrock, W. Singer, M. Tigner, D. Trines, K. Twarowski, G. Weichert, J. Weisend, J. Wojtkiewicz, S. Wolff, and K. Zapfe. "Superconducting TESLA Cavities." *Physical Review Special Topics - Accelerators and Beams* 3.9 (2000): n. pag. Print.
- [8] N. Solyak, I.Gonin, H. Edwards, M.Foley, T.Khabiboulline, D.Mitchell, J.Reid, L.Simmons "Development of the Third Harmonic SC Cavity at Fermilab" Proceedings of the 2003 Particle Accelerator Conference , 0-7803-7739-9 2003 IEEE.
- [9] N. Solyak, H. Edwards, I. Gonin, M. Foley, T. Khabiboulline, D. Mitchell "Development of the 3.9 GHz 3rd Harmonic Cavity at FNAL" FNAL, Batavia, IL 60510, USA
- [10] Ferrario, M., D. Alesini, A. Bacci, M. Bellaveglia, R. Boni, M. Boscolo, M. Castellano, L. Catani, E. Chadroni, S. Cialdi, A. Cianchi, A. Clozza, L. Cultrera, G. Di Pirro, A. Drago, A. Esposito, L. Ficcadenti, D. Filippetto, V. Fusco, A. Gallo, G. Gatti, A. Ghigo, L. Giannessi, C. Ligi, M. Mattioli, M. Migliorati, A. Mostacci, P. Musumeci, E. Pace, L. Palumbo, L. Pellegrino, M. Petrarca, M. Quattromini, R. Ricci, C. Ronsivalle, J. Rosenzweig, A. R. Rossi, C. Sanelli, L. Serafini, M. Serio, F. Sgamma, B. Spataro, F. Tazzioli, S. Tomassini, C. Vaccarezza, M. Vescovi, and C. Vicario. "Direct Measurement of the Double Emittance Minimum in the Beam Dynamics of the Sparc High-Brightness Photoinjector." *Physical Review Letters* 99.23 (2007): n. pag.